Cell, Vol. 87, 307–317, October 18, 1996, Copyright ©1996 by Cell Press

Immunodeficiency and Chronic Myelogenous Leukemia-like Syndrome in Mice with a Targeted Mutation of the ICSBP Gene

Thomas Holtschke,[1,7] Jürgen Löhler,[2,7] Yuka Kanno,[3] Thomas Fehr,[4] Nathalia Giese,[5] Frank Rosenbauer,[6] Jing Lou,[3] Klaus-Peter Knobeloch,[6] Lucia Gabriele,[5] Jeffrey F. Waring,[1] Martin F. Bachmann,[4] Rolf M. Zinkernagel,[4] Herbert C. Morse III,[5] Keiko Ozato,[3] and Ivan Horak[1,6]

[1]Institute of Virology and Immunobiology
University of Würzburg
Würzburg
Federal Republic of Germany
[2]Heinrich-Pette-Institute
University of Hamburg
Hamburg
Federal Republic of Germany
[3]Laboratory of Molecular Growth Regulation
National Institute of Child Health
and Human Development
National Institutes of Health
Bethesda, Maryland 20205
[4]Institute of Experimental Immunology
University of Zürich
Zürich
Switzerland
[5]Laboratory of Immunopathology
National Institute of Allergy and Infectious Diseases
National Institutes of Health
Bethesda, Maryland 20205
[6]Department of Molecular Genetics
Research Institute of Molecular Pharmacology
Krahmerstrasse 6
12207 Berlin
Federal Republic of Germany

Summary

Interferon consensus sequence binding protein (ICSBP) is a transcription factor of the interferon (IFN) regulatory factor (IRF) family. Mice with a null mutation of ICSBP exhibit two prominent phenotypes related to previously described activities of the IRF family. The first is enhanced susceptibility to virus infections associated with impaired production of IFNγ. The second is deregulated hematopoiesis in both ICSBP$^{-/-}$ and ICSBP$^{+/-}$ mice that manifests as a syndrome similar to human chronic myelogenous leukemia. The chronic period of the disease progresses to a fatal blast crisis characterized by a clonal expansion of undifferentiated cells. Normal mice injected with cells from mice in blast crisis developed acute leukemia within 6 weeks of transfer. These results suggest a novel role for ICSBP in regulating the proliferation and differentiation of hematopoietic progenitor cells.

Introduction

Interferon consensus sequence binding protein (ICSBP) is a transcription factor belonging to the interferon (IFN) regulatory factor (IRF) family (Maniatis et al., 1992). This family includes, in addition to ICSBP (Driggers et al., 1992), IRF-1 (Miyamoto et al., 1988), IRF-2 (Harada et al., 1989), ISGF3γ (Veals et al., 1992), and the more recently reported Pip (Eisenbeis et al., 1995) and IRF-3 (Au et al., 1995). These proteins are composed of a conserved DNA-binding domain in the N-terminal region and a divergent C-terminal region that serves as the regulatory domain. The IRF family proteins bind to the IFN-stimulated responsive element (ISRE) and regulate expression of genes stimulated by type I IFNs (IFNα/β). IRF family proteins also control expression of IFNα- and IFNβ-regulated genes that are induced by viral infection (Maniatis et al., 1992). Type II IFN (IFNγ), on the other hand, regulates gene expression primarily through the GAS element, to which Stat1 binds. Stat1 is a component of ISGF3 and is activated by both type I and type II IFNs through janus (JAK) kinases (Darnell et al., 1994). There is extensive cross-talk between ISRE– and GAS–mediated transcription, since ICSBP and IRF-1 are activated by IFNγ, while Stat1 is activated by type I IFN in some cells (Kanno et al., 1993; Pine et al., 1994).

In contrast to IRF-1 and IRF-2, which are expressed in most cells, ICSBP has been shown to be expressed exclusively in cells of the immune system (Driggers et al., 1992). Recent studies show that ICSBP is constitutively expressed throughout B cell ontogeny from early pro-B cells to mature antibody-producing cells. While ICSBP expression is very low in resting T cells and macrophages, its expression is strongly induced in these cells upon immune stimulation and IFNγ treatment. Previous studies have indicated that ICSBP has negative effects on transcription of ISRE–carrying promoters (Nelson et al., 1993, 1996). Furthermore, ICSBP has been shown to complex with IRF-1 and IRF-2 as well as with Pu.1, a member of the Ets family of transcription factors selectively expressed in hematolymphoid cells (Bovolenta et al., 1994; Eisenbeis et al., 1995). In addition to the regulation of IFN-responsive genes, IRF-1 and IRF-2 have been shown to have antioncogenic/oncogenic properties (Harada et al., 1993). Surprisingly, however IRF-1$^{-/-}$ and IRF-2$^{-/-}$ mice do not exhibit gross pathological changes, although a thymocyte developmental defect was noted in IRF-1$^{-/-}$ mice, and IRF-2–deficient animals exhibited abnormalities of bone marrow hemopoiesis and B cell development (Matsuyama et al., 1993).

To investigate the role of ICSBP in vivo, we generated mice with a germline mutation of the ICSBP gene. Here, we report that ICSBP–deficient mice have altered antiviral responses and develop spontaneous disease syndromes with similarities to human chronic myelogenous leukemia (CML). The results suggest that ICSBP, in addition to its role in control of IFN responses, is indispensable for the regulation of hemato- and lymphopoiesis.

Results

Generation of ICSBP–Mutant Mice

The ICSBP gene was mutated by the targeted insertion of a neomycin-resistance gene (PGK-neo) into the second exon (Figure 1), which encompasses the major part

[7]These authors contributed equally to this work.

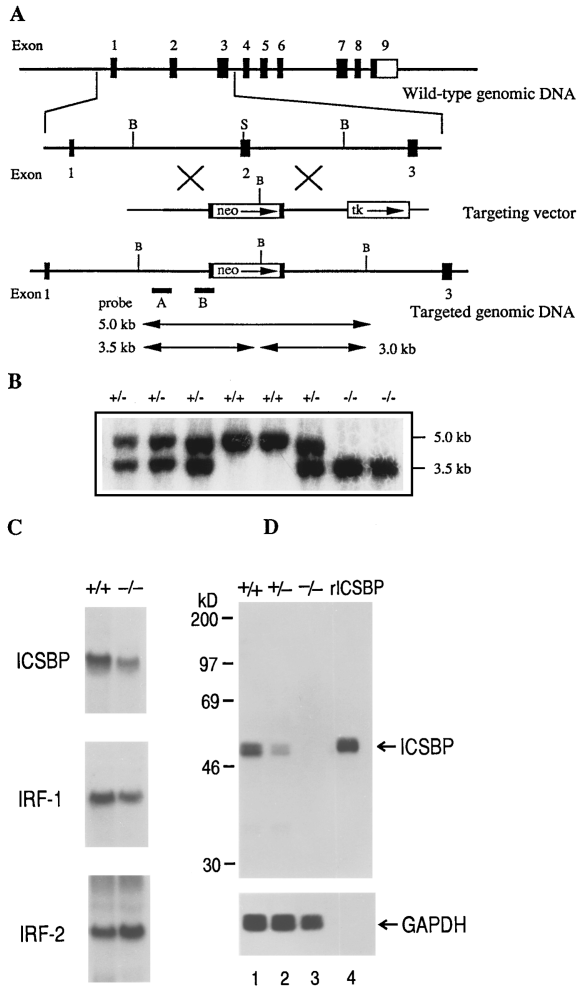

Figure 1. Targeted Disruption of the ICSB Gene

(A) Depicted is the organization of the wild-type ICSBP allele in relation to the targeting vector pPNS-icsbp. The relative positions of the exons are indicated. Closed boxes represent ICSBP coding exons, thick lines represent intron sequences, and thin lines represent bacterial plasmid DNA. The untranslated region of exon 9, the PGK-*neo* and *tk*- cassettes are shown as open boxes. Probes used for Southern blot analysis are shown as closed bars. B, BamHI; S, SmaI. Diagnostic BamHI fragments: a recombinant band, 3.5 kb; a wild-type band, 5.0 kb.

(B) Southern blot analysis of BamHI-digested tail DNA of F_2-offspring. The DNA was hybridized with the probe A.

(C) Northern blot analysis shows splenic RNA (20 μg) hybridized with labeled ICSBP, IRF-1, and IRF-2 cDNA probes (Kanno et al., 1993).

(D) Immunoblot analysis of ICSBP expression in spleens of mutant mice. Whole cell extracts (40 μg) were separated on 10% SDS–polyacrylamide gel electrophoresis, and immunoblot analysis was performed using rabbit anti–ICSBP antibody (Bovolenta et al., 1994). Baculovirus recombinant ICSBP (10 ng) was used as a control. Levels of GAPDH (lower panel) in whole cell extracts were monitored to ensure equal protein loading (Nelson et al., 1996). As expected, no GAPDH immunoreactivity was present in the recombinant ICSBP preparation (right lane).

of the DNA-binding domain. ICSBP–mutant mice were derived as described in Experimental Procedures. Progeny of crosses from mice heterozygous for the mutation yielded the expected proportions of genotypes.

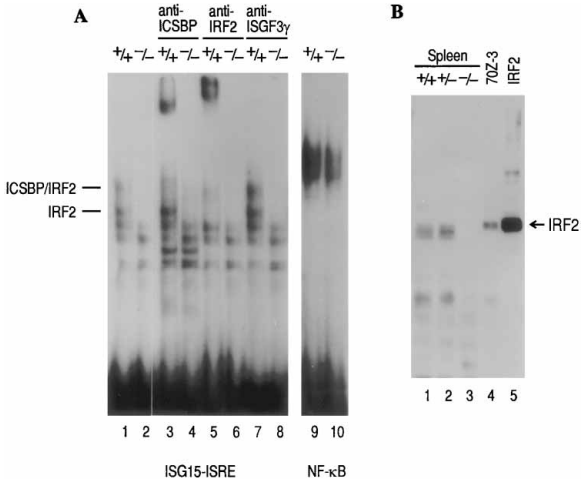

Figure 2. The Absence of the ICSBP–IRF-2 Complex

(A) Electrophoretic mobility shift assay analysis of ISRE-binding activity. Nuclear extracts (10 μg of protein) from ICSBP$^{+/+}$ and ICSBP$^{-/-}$ spleens were tested for ISRE-binding activity using ^{32}P-labeled ISG15 probe (Bovolenta et al., 1994). Extracts were incubated with preimmune rabbit serum (lanes 1 and 2), anti–ICSBP antibody (lanes 3 and 4), anti–IRF-2 antibody (lanes 5 and 6), and anti-ISGF3γ antibody (lanes 7 and 8) for 15 min prior to the addition of the probe. As a control, the same extracts were analyzed with a NFκB probe (Kanno et al., 1993; lanes 9 and 10).

(B) Immunoblot analysis was performed for IRF-2 with 30 μg of nuclear extracts, using rabbit anti–IRF-2 antibody as described (Nelson et al., 1996). Nuclear extracts from pre-B cells (70Z-3) and in vitro translated IRF-2 were used as positive controls (right).

Northern blot analysis of poly(A)$^+$RNA isolated from spleens of ICSBP$^{-/-}$ mice revealed a single ICSBP mRNA species slightly shorter than that from ICSBP$^{+/+}$ mice (Figure 1). The sequence analysis of corresponding cDNA confirmed a short insert from the neo cassette gene and, as a result, the reading frame disruption by multiple stop codons (data not shown). In agreement with these results, no ICSBP protein was detected by immunoblot analysis of spleen cell extracts from ICSBP$^{-/-}$ mice (Figure 1E). Also noted were the consistently lower levels of ICSBP protein in extracts from ICSBP$^{+/-}$ mice as compared with those from ICSBP$^{+/+}$ mice, indicating a gene dosage effect of ICSBP expression. Predictably, IRF-1 and IRF-2 mRNA levels in ICSBP$^{-/-}$ spleen were similar to those found in control mice (Figure 1D).

Absence of the ICSBP–IRF-2 Complex

To examine whether ISRE–binding activity was altered in ICSBP$^{-/-}$ mice, we performed electrophoretic mobility shift assay analysis with nuclear extracts from spleen. There were five bands in control extracts, of which the two upper bands were missing in extracts from the ICSBP$^{-/-}$ spleen (Figure 2A, lanes 1 and 2). In vivo, ICSBP occurs as a complex with IRF-2 (Nelson et al., 1996), which is represented by the uppermost band that was supershifted by anti–ICSBP antibody (lane 3). However, no supershifted band was detected in extracts from the ICSBP$^{-/-}$ spleen (lane 4), consistent with the absence of the ICSBP protein in ICSBP$^{-/-}$ spleen cells. Anti–IRF-2

antibody supershifted the two uppermost bands in control extracts (lane 5), which consisted of, first, the ICSBP–IRF-2 complex and second, IRF-2. However, anti–IRF-2 antibody did not supershift a band in ICSBP$^{-/-}$ extracts (lane 6), indicating that IRF-2 expression is deficient in ICSBP$^{-/-}$ mice. As seen in the immunoblot analysis (Figure 2B), the IRF-2 protein was not detected in ICSBP$^{-/-}$ spleen extracts, consistent with the absence of IRF-2 binding. Anti–ISGF3γ antibody, used as a control, did not supershift a band in extracts from either ICSBP$^{-/-}$ or wild-type mice (Figure 2A, lanes 7 and 8). A control probe containing the binding site for NFκB produced a similar binding pattern with extracts from both ICSBP$^{+/+}$ and $^{-/-}$ mice, confirming the specific abrogation of the ICSBP–IRF-2 complex in the ICSBP$^{-/-}$ mice.

Our data suggest that IRF-2 protein expression is reduced in ICSBP$^{-/-}$ spleen (Figure 2B), the basis of which is currently under study. The fact that a considerable amount of IRF-2 mRNA was detected in ICSBP$^{-/-}$ spleen suggests a defect in posttranscriptional/translational modifications of IRF-2. It has been shown previously that enhanced C-terminal cleavage of IRF-2 occurs in virus-infected cells (Palombella and Maniatis, 1992).

Expression of IFN–Regulated Genes

Since IFNα and IFNβ genes carry the ISRE in their promoters and their expression is regulated by the IRF family proteins, we performed reverse transcriptase–polymerase chain reaction (RT–PCR) analysis for expression of these genes in spleen, lymph nodes, and bone marrow. Constitutive IFNα and IFNβ mRNA levels were not grossly altered in ICSBP$^{-/-}$ tissues (data not shown). Furthermore, although ICSBP is known to affect activity of MHC class I and β2-microglobulin promoters (Nelson et al., 1993), no significant alterations were detected in their mRNA levels or the surface expression of MHC class I on ICSBP$^{-/-}$ lymphoid cells (data not shown).

In addition, we observed that spleen cells from ICSBP$^{-/-}$ mice respond to both IFNα and IFNγ in vitro by activating ISGF3γ and Stat1, indicating that the pathways for JAK/Stat and JAK/ISGF3γ are not abrogated in ICSBP$^{-/-}$ spleen cells (data not shown).

Immune System and Cytokine Expression of ICSBP$^{-/-}$ Mice

To determine whether hematopoietic development is affected by the absence of ICSBP, we compared spleen, bone marrow, lymph node, and thymus cells for expression of cell lineage markers by flow cytometric analyses (Figure 3).

The most striking finding was markedly increased frequencies of granulocytes (GR-1$^+$/Mac-1$^+$) and, to a lesser extent, macrophages (GR-1$^-$/Mac-1$^+$) in spleen, lymph node, and bone marrow (Figure 3A). Markedly increased frequencies of granulocytes were also detected in peripheral blood (see below). The frequencies of granulocytes in spleen and nodes of homozygous deficient mice were found to increase with age.

Although the relative frequencies of B cells and T cell subsets were decreased in spleen (Figure 3A), the total numbers of lymphocyte subsets were either normal (CD4$^+$ and CD8$^+$ T cells) or increased 2-fold or more (B cells) owing to the proportionate increases in spleen size and cellularity. In lymph nodes, the frequency of B cells was significantly increased, and the proportion of mature B cells with the phenotype of plasmablasts (B220^{dull}, CD43$^+$) in both spleen and lymph node was augmented relative to that of small resting cells. Correspondingly, increased levels of serum Ig were detected (data not shown). The population of CD5$^+$ B cells in the peritoneal cavity was not detectably expanded (data not shown). For ICSBP–deficient mice, the organization and cellular composition of the thymus were essentially normal, with both immature CD4$^+$CD8$^+$ and mature single positive CD4$^+$CD8$^-$ and CD4$^-$CD8$^+$ cells present in normal frequencies (data not shown). This indicates that early T cell development and selection is grossly normal in mice lacking ICSBP.

The ability of T cells or NK cells to produce IFNγ was examined following stimulation of spleen cells with ConA or lipopolysaccharide (LPS; Figure 3B). IFNγ production in response to ConA was reduced more than 3-fold in ICSBP$^{-/-}$ mice 1–5 months of age, while IFNγ production in response to LPS was reduced more than 100-fold compared with ICSBP$^{+/+}$ mice; indeed, responses were below the limits of detection in 9 of 12 ICSBP$^{-/-}$ mice. RT–PCR analyses of constitutive IFNγ transcripts showed them to be reduced about 3-fold in spleens of ICSBP$^{-/-}$ as compared with wild-type animals (Figure 3C). For ICSBP$^{-/-}$ mice, the levels of IFNγ protein induced by ConA and the steady-state levels of transcripts for IFNγ are in keeping with the reduced relative frequencies of T cells in spleen and suggest that IFNγ expression by T cells is normal.

Expression of IFNγ following activation of spleen cells with LPS is induced by IL-12 produced primarily by macrophages and monocytes and, to a lesser extent, B cells and neutrophils. The possibility that decreased IFNγ expression in ICSBP$^{-/-}$ mice following LPS stimulation could be due to altered regulation by IL-12 was suggested by the observation that transcripts for the p40 chain of this cytokine were markedly reduced in spleens of mutant mice, while expression of IL-12 p35 transcripts was normal (Figure 3B). The deficiency in IL-12 p40 expression is quite striking considering the increased frequencies of macrophages and monocytes in spleens of mutant mice.

Antiviral Immune Responses

Immune responses of ICSBP$^{-/-}$ mice to three different viruses were analyzed. ICSBP$^{-/-}$ mice survived and were able to produce normal neutralizing antibody titers to vesicular stomatitis virus (VSV), suggesting that the B and T helper cell compartment as well as the IFN type I system were normal in these mice (data not shown). However, when ICSBP$^{-/-}$ mice were infected with vaccinia virus (VV) or lymphocytic choriomeningitis virus (LCMV) at a dose that was well controlled by normal littermates, 80% of VV–infected and 100% of the mice infected with the slowly and restrictedly replicating LCMV strain Armstrong died within 10–20 days (Figures 4C and 4G). Analysis of cytotoxic T lymphocyte (CTL) responses after VSV (Figure 4A, secondary restimulation

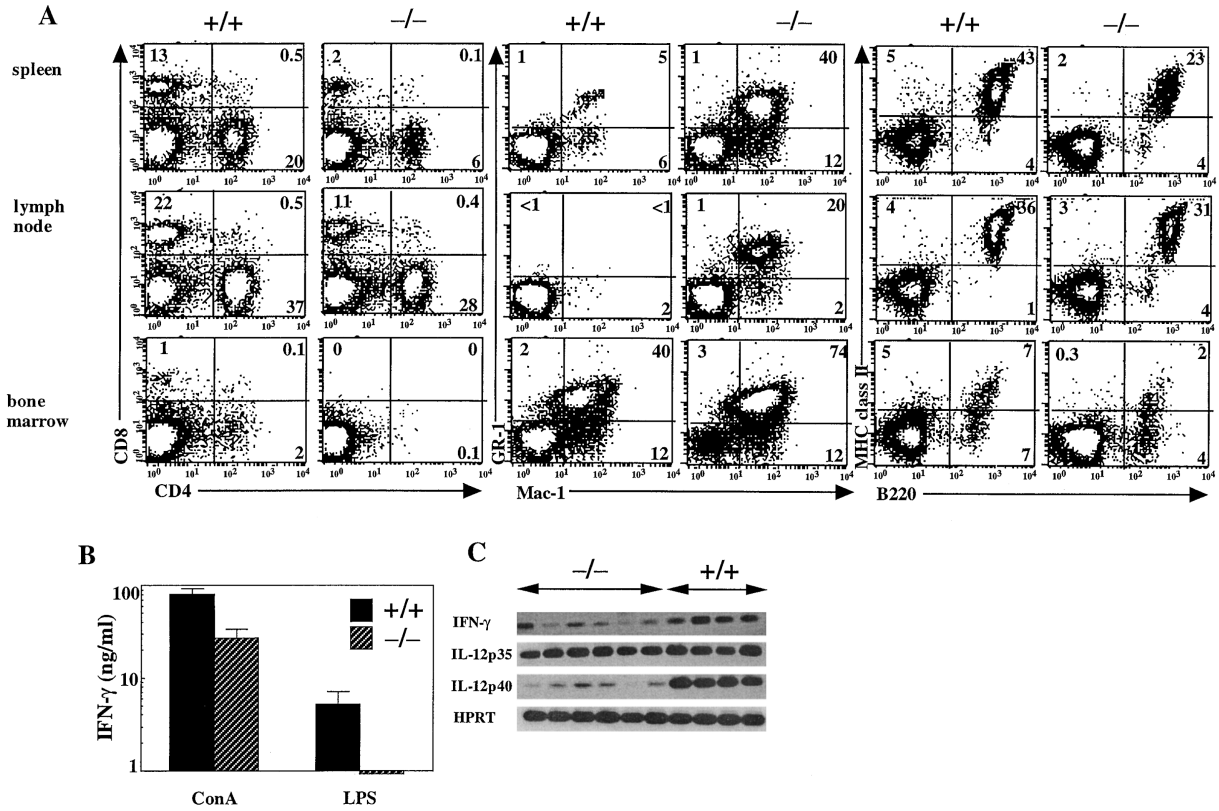

Figure 3. Immunologic Features of ICSBP$^{-/-}$ Mice

(A) Single cell suspension from spleen, bone marrow, lymph node, and thymus of ICSBP–deficient mice (−/−) and their wild-type littermates (+/+) were stained with indicated combinations of antibodies for flow cytometric studies. Numbers in the quadrants indicate the percent among total cells in the quadrant. Analyses were of 11-week-old mice and are representative of five pairs of +/+ and −/− mice tested at 10–16 weeks of age. For mice in this age range, the weights and total cellularity of ICSBP$^{-/-}$ spleens were increased 3- to 5-fold over controls, and lymph node size and cellularity were increased 2- to 3-fold over normal.

(B) ConA- and LPS-induced IFNγ expression by spleen cells was determined by enzyme-linked immunosorbent assay. Results indicate the mean plus or minus standard error for assays of 10 +/+ and 12 −/− mice.

(C) RTR–PCR analyses of constitutive IFNγ, IL-12p35, IL-12p40, and HPRT transcripts in spleen cells of ICSBP–deficient (−/−) and wild-type littermate controls (+/+).

d33) and VV infection (Figure 4B, primary response d6) revealed a 3- to 10-fold reduction of CTL activity. These data suggested an enhanced virus replication in the early phase, which then could not be controlled by the later developing specific CTL responses. To test this, we infected ICSBP$^{-/-}$ mice with 200 pfu of the rapidly and widely replicating LCMV strain WE. While infection into the footpad was well controlled by the virtually normal CTL responses (Figure 4D), intravenous infection caused death of about 40% of the animals (Figure 4G); this was most likely due to immunopathology, as documented by CD8$^+$ T cell–mediated hepatitis (Figure 4H; Zinkernagel et al., 1986). The other 60% survived owing to exhaustion of the specific CTL response (Moskophidis et al., 1993) and uninhibited growth of LCMV-WE. This was shown by markedly reduced primary and absence of secondary CTL responses (Figures 4E and 4F) and persisting virus in liver (1×10^5 pfu), spleen (7×10^6 pfu), and kidney (8×10^5 pfu) 40 days after infection.

CML–like Disease

Although young ICSBP$^{-/-}$ mice showed no difference in size, behavior, and reproductive ability as compared with wild-type littermates, they developed with a 100% penetrance signs of a hematologic neoplasia with a resemblance to CML in humans. Macroscopically, the most prominent alteration was a systemic lymphadenopathy and hepatosplenomegaly. The enlarged lymph nodes were colonized by neutrophilic granulocytes (Figure 5A), predominantly mature neutrophils intermingled with juvenile and myelocytic forms. Paracortical and medullary plasma cell hyperplasia, at least temporarily, also contributes to lymph node enlargement. Pseudo-Gaucher cells phagocytosing granulocytic and other hematopoietic cells were abundant (Figure 5B). The plasma cells were chiefly of the IgG isotype and displayed cytomorphological anomalities usually encountered in plasmacytomas (Figure 5C). The progressive expansion of myeloid, histiocytic, and B-lymphoid cells leads finally to complete effacement of lymph node architecture.

In mice, in contrast to humans, the spleen is a hematopoietic as well as a lymphoid organ. In ICSBP$^{-/-}$ mice, a progressive expansion of the red pulp was seen with increasing age comprising the same cell types observed in the lymph nodes of the mutant mice. In addition,

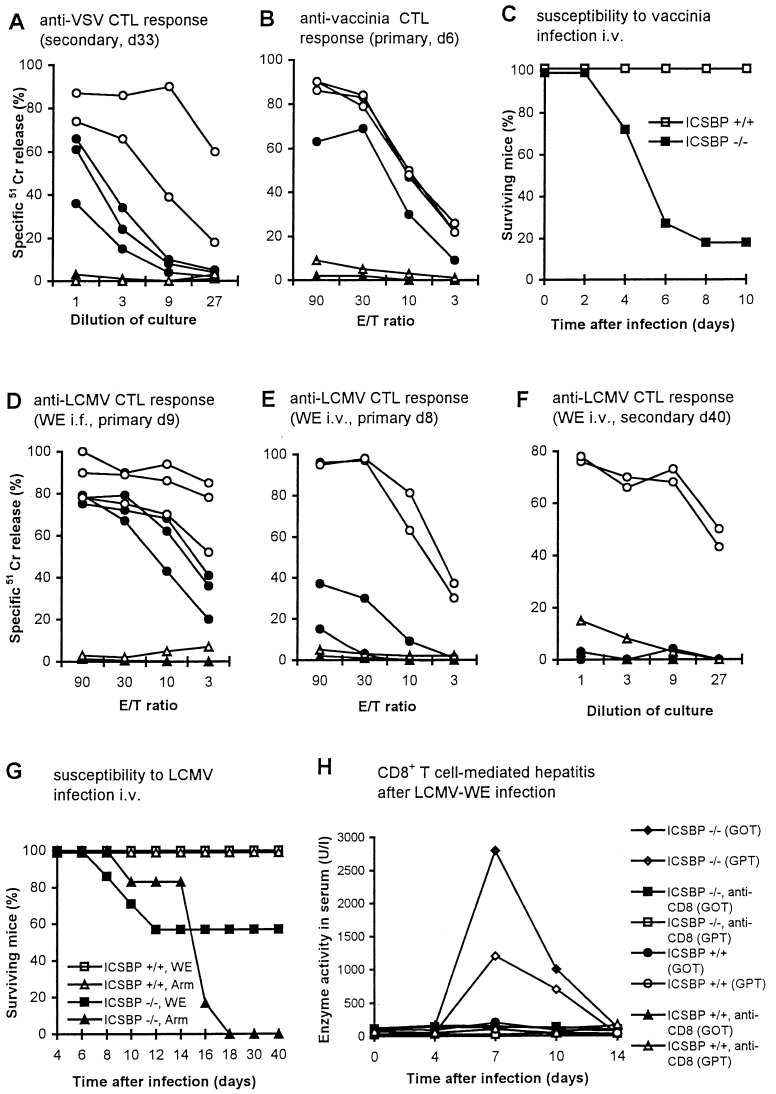

Figure 4. Antiviral Immune Responses of ICSBP$^{-/-}$ Mice

(A and B, D–F) Mice were infected with the respective viruses on day 0, and primary ex vivo or secondary in vitro (after 5 days of restimulation) activity of CTLs was determined in Cr-release assay on peptide-loaded (VSV and LCMV) or virus-infected (VV) target cells. E/T ratio, effector to target cell ratio; i.v., intravenously; i.f., into the footpad. Open symbols: ICSBP$^{+/+}$ mice; closed symbols: ICSBP$^{-/-}$ mice; circles: peptide-pulsed or virus-infected target cells; triangles: unlabeled target cells. Each line represents one mouse. One of two comparable experiments of each type is shown.

(C and G) Mice were infected with 2×10^6 pfu of VV (C, n = 11) or 2×10^2 pfu of the LCMV isolates WE or Arm (G, n = 7 or 6, respectively), and survival was monitored during the indicated time periods. Open symbols: ICSBP$^{+/+}$ mice; closed symbols: ICSBP$^{-/-}$ mice.

(H) Mice were infected with 200 pfu of LCMV-WE on day 0 with or without prior in vivo depletion of CD8$^+$ T cells, and the occurence of hepatitis was monitored by determination of liver enzyme activity in serum on the indicated timepoints. Closed symbols: glutamate oxalacetate aminotransferase (GOT); open symbols: glutamate pyruvate aminotransferase (GPT) activity.

erythropoiesis was greatly increased, and there was a marked proliferation of abnormal megakaryocytes.

Myeloproliferative alterations of bone marrow and lymphoid tissues precede changes in the composition of blood leukocytes for a long time. Only when the spleen has tripled its normal size can a significant shift towards the granulocytic lineage be recorded. Examination of blood films of ICSBP$^{-/-}$ mutants with fully developed myeloproliferative disease, which is associated with moderately elevated leukocyte numbers, revealed left-shifted neutrophilia (Table 1). Morphologically, the white blood cells at this disease stage appeared mostly normal (Figure 5D).

The bone marrow of ICSBP$^{-/-}$ mice exhibited a marked hypercellularity due to an increase of mature granulocytes and their precursors (Table 1; Figure 5E) intermingled with numerous pseudo-Gaucher cells. The frequencies of lymphocytes and plasma cells were reduced. The erythroid compartment was greatly decreased, and megakaryocytes were atypical and with advanced disease reduced numerically. Evolution of fibrosis was not observed, but, consistently, the connective tissue of the periosteum and adjoining musculature was invaded by myeloid cells. Involvement of liver characterized by extensive periportal and sinusoidal invasion by mature and immature granulocytes and pseudo-Gaucher cells, similar to leukemic liver infiltration in humans, is an invariant characteristic of ICSBP–deficient animals, as is the granulocytic and plasma cell infiltration of myocardium, lungs, and kidneys. A moderate numerical increase of hypertrophic mast cells is seen in the loose connective tissue. In the small intestine there is a striking hyperplasia of lymphocytes and plasma cells in Peyer's patches and the lamina propria. In summary, the hematologic alterations in ICSBP$^{-/-}$ mice are mainly characterized by hyperproliferation of abnormal myeloid, histiocytic, and lymphocytic cells, which in some aspects simulates the chronic phase of CML in humans.

Similar hematopathologic alterations, although in a quantitatively reduced form, were observed also in ICSBP$^{+/-}$ mice (data not shown).

Fatal Blastic Leukemia

Transition of the chronic form to fatal blast crisis is a characteristic feature of human CML. Approximately

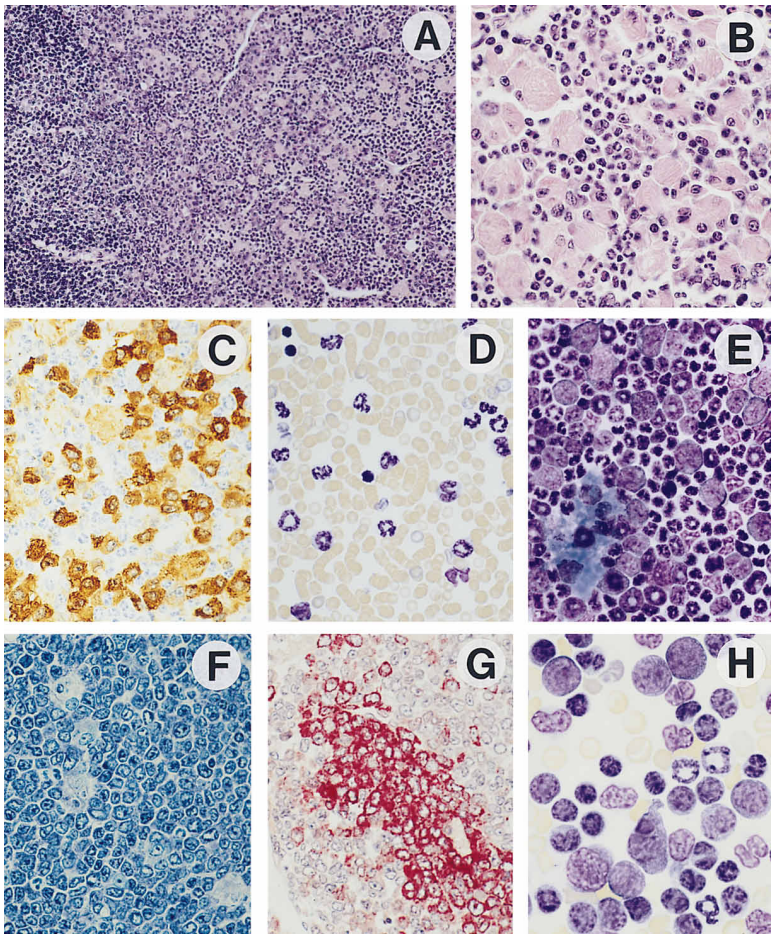

Figure 5. Hematopathology of ICSBP$^{-/-}$ Mice

(A) Enlarged peripheral lymph node with residual cortical follicle and germinal center on the left side. Paracortex and medulla are densely populated with neutrophils, eosinophilic pseudo-Gaucher cells, and plasmablasts (hematoxylin–eosin, × 100).

(B) Pseudo-Gaucher cells in lymph node exhibit intracellular storage of crystaloid, eosinophilic material, and hemophagocytosis. Notice absence of lymphocytes; instead, many granulocytes and some plasma cells are present (hematoxylin–eosin, × 530).

(C) Hypertrophic atypical plasma cells of lymph node medulla (IgG immunostaining, × 400).

(D) Blood film of ICSBP–deficient mouse showing neutrophilic leukocytosis (Pappenheim stain, × 400).

(E) Bone marrow smear demonstrating increase of granulopoiesis while erythropoiesis is absent. A pseudo-Gaucher cell is seen in the lower left corner (Pappenheim stain, × 400).

(F) Granulocytic sarcoma of lymph node during blast cell crisis consisting of relatively uniform medium-sized myeloid blast cells (Giemsa stain, × 530).

(G) Leukemic infiltration of kidney during blast cell crisis. Most of the tumor cells stain positive (red) by myeloperoxidase immunostaining (× 500).

(H) Blood film depicting severe leukocytosis composed of myeloid and lymphoid blast cells besides atypical monocytoid cells and some normal lymphocytes and neutrophils (Pappenheim stain, × 825).

33% of ICSBP$^{-/-}$ and 9% of ICSBP$^{+/-}$ mice became moribund by 50 weeks of age (Figure 6A); all moribund mice had features indicating a transition to a blast crisis.

Macroscopically, the changed course of disease process is characterized by striking lymphadenopathy and hepatosplenomegaly (spleen weight 500–2000 mg) and

Table 1. Hematological Parameters of CML-like Disease (Chronic Stage) in ICSBP–Deficient Mice

	Peripheral blood		Bone marrow	
ICSBP	+/+[b]	−/−[c]	+/+[d]	−/−[e]
	Percent of cells[a]			
netrophil segments	11.75 ± 1.8	58.0 ± 6.5	29.02 ± 3.61	58.1 ± 3.26
netrophil bands	0.25 ± 0.25	1.17 ± 0.79		
metamyelocytes	<0.03	1.0 ± 0.69	2.9 ± 0.6	7.95 ± 1.59
myelocytes			8.34 ± 0.84	7.65 ± 0.45
promyelocytes	<0.03	0.14 ± 0.14	3.37 ± 0.5	6.77 ± 0.33
myeloblasts			1.1 ± 0.13	5.9 ± 0.21
eosinophils	2.5 ± 0.63	1.43 ± 0.37	3.55 ± 0.7	1.52 ± 0.13
lymphocytes	84.5 ± 1.66	28.71 ± 4.16	25.37 ± 1.79	7.19 ± 2.19
lymphoblasts	<0.03	0.71 ± 0.29		
nuclear erythroid cells	<0.03	<0.03	25.14 ± 2.31	4.38 ± 1.1
megakaryocytes	<0.03	<0.03	0.42 ± 0.14	<0.05
monocytes	1.25 ± 0.48	2.43 ± 1.48	1.19 ± 0.28	1.39 ± 0.38
leukocytes/μl × 10^3	6.76 ± 0.55	38.9 ± 9.5		
erythrocytes/μl × 10^6	8.65 ± 0.71	7.89 ± 0.48		
platelets/μl × 10^5	9.22 ± 0.75	12.30 ± 1.07		

[a] Differential cell counts were performed by identifying at least 300 cells per peripheral blood smear and 500 cells per marrow smear. Numbers are given as means plus or minus standard error.
[b] n = 4, [c] n = 7, [d] n = 3, [e] n = 3

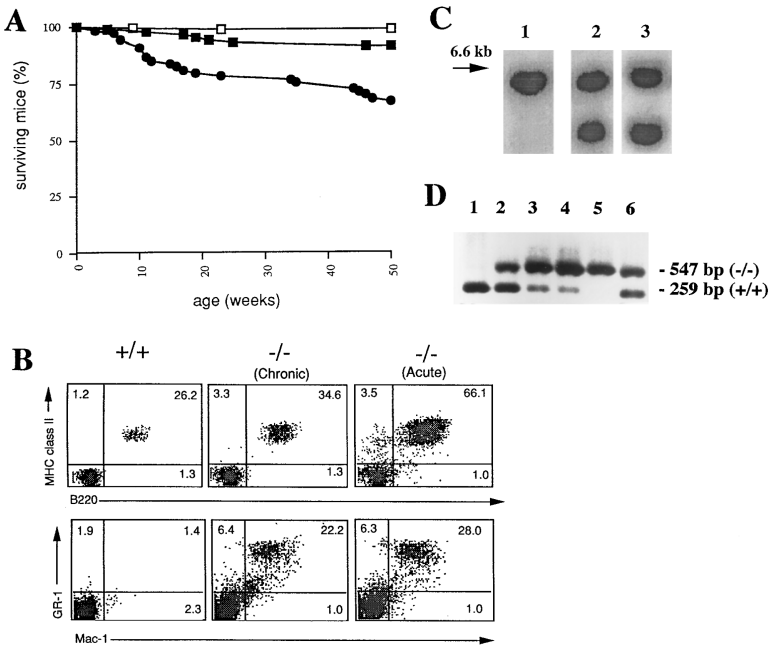

Figure 6. Fatal Blastic Leukemia

(A) Mortality of ICSBP$^{-/-}$ (circles), ICSBP$^{+/-}$ (closed squares), and ICSBP$^{+/+}$ (open squares) mice.

(B) FACS analysis of cells from +/+ and −/− mice from chronic and acute stage of disease. Lymph node cellls were stained with indicated combinations of antibodies and analyzed as described in Experimental Procedures. The ages of the mice were 36 weeks for the +/+ and 25 and 22 weeks for the −/− mice in chronic or acute stage, respectively. The weights and total cellularity of −/− lymph nodes were increased 5-fold over control for the chronic stage and 18 times over control for the acute stage.

(C) Clonal expansion of leukemic cells. Southern blot hybridization for the organization of IgJ_H genes using J_H probe. DNA prepared from the spleen of a 10-month-old ICSBP$^{-/-}$ mouse in blastic stage (lane 1) or two recipients of spleen cells (lane 2) or lymph node cells (lane 3) from another ICSBP$^{-/-}$ mice in blastic stage.

(D) Determination of the genotype of tumor cells in ICSBP$^{+/+}$ mice transplanted with cells from ICSBP$^{-/-}$ mice in blastic stage. DNA samples from tissues of a leukemic recipient (lanes 2, 3, 4, and 6) and control ICSBP$^{+/+}$ (lane 1) and ICSBP$^{-/-}$ (lane 5) mice were analyzed by PCR using primers described in Experimental Procedures. Tissues of a leukemic recipient: ear (lane 2), spleen (lane 3), solid tumor (lane 4), liver (lane 6).

additionally by a marked enlargement, distortion, and greenish-white hue of all abdominal organs, including the intestinal and urogenital tracts. On microscopic inspection, the organ lesions are characterized by a diffuse uniform infiltrate of medium-sized or blast cells (see Figure 5F) focally intermingled with some myeloid and histiocytic cells of different maturational stages and, in the case of lymph node tumors, with residual lymphocytes. Sometimes eosinophils are interspersed among the blast cells. Although the blast cells with their round or, less frequently, irregular nuclei and scanty cytoplasm mimic lymphoblastic or mixed cell lymphomas, their staining for myeloperoxidase (Figure 5G), chloroacetate esterase, lysozyme, and immunoglobulins revealed that most of them belong to the granulocytic lineage; but areas of histiocytic and lymphocytic differentiation are also present. These findings in the nonhematopoietic tissues are equivalent to what in human blast cell crisis is designated as granulocytic sarcoma or chloroma. Hematologically, this stage of the disease is characterized by leukocyte counts of over 100,000 per μl with a blast prevalence of about 10% and a prevalence of atypical neutrophils of about 14%, while lymphoid cells accounted for about 76% (Figure 5H). Immunostaining of blood films revealed that only half of the blasts were Mac-1$^+$, indicating a bi- or tri-phenotypic nature of the blast transformation. Expansion of both granulocytic and B-lymphoid cells has also been documented by fluorescence-activated cell sorter (FACS) analyses (Figure 6B). Histologically, the bone marrow is populated by a relatively uniform mass of blasts and immature myeloid cells eroding the bone and invading and replacing the adjoining musculature. A typical myelogram consists of 30.4% greatly abnormal myeloblasts, promyelocytes, myelocytes, and metamyelocytes, 58.5% atypical neutrophils, 4.5% erythroid cells, 4.1% lymphoid cells, 0.9% eosinophils, and 1.6% Gaucher-like cells or sea-blue histiocytes.

Transplanted Leukemias

To test the leukemogenicity of cells from both chronic stage and blast crisis, 1×10^6 cells were injected intravenously into nonirradiated ICSBP$^{+/+}$ mice. As shown in Table 2, 15 of 16 mice injected with cells from two mice in blast crisis developed progressively growing leukemias within 6–11 weeks of transplantation. By contrast, only 1 of 62 mice injected with cells from 10 mice in the chronic phase of disease developed a leukemia of donor origin.

The transplanted cells developed in the hematopoietic, lymphoid, and parenchymal organs of their hosts into the same kind of leukemia and widespread granulocytic sarcomas with mixed differentiation as in the ICSBP$^{-/-}$ donors with blast crisis. Accordingly, in all diseased recipient animals with granulocytic sarcomas, Pappenheim-stained bone marrow smears consisted exclusively of 50% small atypical lymphoid cells and 50% small to medium-sized blasts, a portion of which exhibited some myeloid differentiation (azurophilic granules). In the periphery, the leukemic blood (greater than 100,000 leukocytes per μl) contained 12.1% blast cells, atypical promyelocytes, and myelocytes, 7.6% atypical neutrophils, and 79.8% lymphoid cells. Expression of leukocyte markers was in a representative case 49% Ia$^+$(B cells), 31% Mac-1$^+$ (myeloid and monocytic cells), and 11% Thy-1$^+$ (T cells).

Southern blot analyses of immunoglobulin heavy chain gene J_H organization showed the transplanted cells to be clonal (Figure 6C). Furthermore, the origin of leukemic clones from donor mice was confirmed by

Table 2. Transplantable Leukemias

Disease-stage of donors	Donor organ	Number of donors	Number of recipients	Observation time (weeks)	Number of recipients with leukemia
chronic	sp	6	28	11–12	1
chronic	bm	4	34	11–23	0
blast crisis	sp	2[a]	10	6–11	9
blast crisis	bm	1[a]	3	6	3
blast crisis	ln	1[a]	3	6	3

Nonirradiated ICSBP$^{+/+}$ mice were injected i.v. with 10^6 cells from lymphoid organs of ICSBP$^{-/-}$ mice. Mice were scored for the development of leukemia by blood smears. Abbreviations: sp, spleen; bm, bone marrow; ln, lymph nodes.
[a] The same mouse was used as a donor.

PCR analyses revealing the presence of 547 bp band diagnostic of ICSBP$^{-/-}$ cells (Figure 6D).

The possibility that ecotropic retroviral insertional mutagenesis might be involved in the genesis of the leukemias is ruled out by two observations. First, mice with the ICSBP mutation bred onto the 129 genetic background, which lacks endogenous ecotropic virus, develop changes like those seen on the (129 × C57BL/6) mixed genetic background. Second, neither germline nor acquired clonal ecotropic proviral integrations were detected by Southern blot analyses of the DNAs from leukemia transplants found to have clonal J_H rearrangements (data not shown).

Discussion

The above results reveal two main features of ICSBP–deficient mice. They are more susceptible to certain virus infections, and they develop a myelolymphoproliferative disease with similarities to human CML. These findings suggest that ICSBP plays two distinct roles: first, as a prominent regulator of antiviral immune responses, and second, as a critical growth determinant of hematopoietic cells.

Immunodeficiency

The humoral arm of the antiviral response to VSV was found to be intact, indicating relatively normal T helper cell–B cell interactions. Dramatically enhanced viral replication in the early phase of infection, probably due to an IFNγ–dependent defect in innate immunity, overhelmed the reduced but still sufficient CTL responses. The outcome was death due to virus-induced tissue destruction in the case of cytopathic VV or changed quality of immunopathology in the case of the restrictedly replicating noncytopathic variant (Arm) of LCMV. For VSV and peripheral infections with LCMV-WE, the phenotype of ICSBP$^{-/-}$ mice corresponds to IFN type II receptor-deficient mice (Huang et al., 1993); for systemic infection with LCMV-WE, the phenotype with viral persistence is intermediate between IFN types I and II receptor-deficient mice (Müller et al., 1994). Similarly impaired antiviral immunity was seen previously in IRF-2–deficient mice, which died within 30 days of intravenous infection with LCMV (Arm), a challenge survived normally by IRF-1–deficient and normal mice (Matsuyama et al., 1993).

The marked reduction in transcripts for IL-12(p40) suggests that ICSBP and its interactions with other members of the IRF family may be critical determinants of IL-12 expression and thus may influence production of IFNγ as well as the balance of CD4$^+$ T helper 1 to T helper 2 function in immune responses to a variety of pathogens (Trinchieri, 1995).

Induction of IFNγ appears critical for resolving these infections, and ICSBP$^{-/-}$ mice are deficient in production of this cytokine following stimulation of T cells by cross-linking of the T cell receptor (TCR) or B cells and macrophages with LPS. The way in which ICSBP regulates expression of the IFNγ gene is not known, but direct effects on gene transcription are unlikely, since an ISRE or a similar element has not been identified in the regulatory regions of the gene. The role of ICSBP in IFNγ regulation is more likely indirect and could reflect the influences of ICSBP on IL-12 or other elements of the cytokine network, which may be perturbed in ICSBP$^{-/-}$ mice.

A further indication of an impaired immune system is a high susceptibility of ICSBP$^{-/-}$ mice kept in a conventional facility to opportunistic infections, which frequently manifest as chronic purulent skin ulcerations and pseudotumorous botryomycosis (data not shown).

The Role of ICSBP in Early Hematolymphoid Progenitors

A central conclusion to be drawn from these studies is that ICSBP–deficient mice exhibit enhanced proliferation of myeloid, monocytic, lymphoid, and perhaps megakaryocytic lineages, suggesting that the decisive alteration occurs in an early common progenitor cell. Effects of the ICSBP mutation were evident already by day 17 of embryogenesis (data not shown), supporting the notion that the defect is not caused by environmental factors but by an alteration in the developmental potential of a stem cell common to these lineages.

Development of hematolymphoid cells from pluripotent stem cells proceeds through a tightly controlled process of differentiation and proliferation of immature lineage-committed progenitors into fully mature cells. On the molecular level, this control is exercised by networks of extracellular and intracellular signaling pathways, which regulate expression of specific target genes (for review see Metcalf, 1989; Weissman, 1994). Recently, several transcription factors essential for hematopoietic development such as Tal-1, Rbtn-2, GATA-1 and 2, Pu.1, and others were identified by targeted mutagenesis. The exact in vivo role for most of these factors and their target genes, however, remains to be elucidated (for review see Shivdasani and Orkin, 1996).

ICSBP seems to regulate negatively a critical growth-control gene and could thus be a tumor suppressor. This is not surprising in view of the described oncogenic/antioncogenic activity of other IRF genes (Harada et al., 1993). Furthermore, a monocytic cell line transfected with a dominant negative form of ICSBP exhibited altered growth (Thornton et al., 1996; our unpublished data).

Changes in the normal pattern of cytokine signaling would be an obvious explanation for the hematopoietic abnormalities seen in ICSBP–deficient mice. For example, it has been shown that overexpression of IL-3, IL-6, or GM-CSF can cause myeloproliferation in mice (Wong et al., 1989; Hawley et al., 1992; Johnson et al., 1989). In ICSBP$^{-/-}$ mutants, semiquantitative RT–PCR analyses do not reveal substantial (greater than 3-fold) differences in expression of splenic transcripts for IL-1, IL-2, IL-3, IL-4, IL-5, IL-6, IL-10, IL-12(p35), IFNα1, IFNβ, TNFα, G-CSF, GM-CSF, or LIF (data not shown). However, transcripts for several cytokine receptors, G-CSFR, GM-CSFR, and M-CSFR, were reduced in granulocytes of ICSBP$^{-/-}$ as compared with wild-type mice (data not shown). The importance of these quantitative changes to the alterations in myelopoiesis observed in ICSBP$^{-/-}$ mice is not yet known.

Nevertheless, the fact that we have not observed any dramatic changes in cytokine expression, except for IFNγ and IL-12, does not exclude the possibility that cytokine signaling pathways could be altered in ICSBP$^{-/-}$ mice.

CML–like Disease

The major characteristic features of human CML (first, a chronic period of disease with predominantly granulocytic involvement; second, transition into a fatal blast crisis with the clonal expansion of undifferentiated cells; and third, the involvement of several cell lineages indicative of a defect in an early common progenitor) are invariably found in the murine disease as well.

The molecular hallmark of CML is the presence of an activated bcr–abl tyrosine kinase resulting from a t(9;22) chromosomal translocation originally identified as the Philadelphia chromosome. Several mouse model systems involving expression of the bcr–abl fusion protein have demonstrated a causal relationship with the development of myeloid and lymphoid malignancies (reviewed by Sawyers et al., 1991). Multiple downstream targets of the bcr–abl or abl are suggested by different studies that include ras as well as Jak/STAT signaling (Danial et al., 1995; Carlesso et al., 1996). Analyses of abl mRNA expression and the genomic organization of c-abl in ICSBP$^{-/-}$ mice did not reveal any differences as compared with control mice (data not shown). Nevertheless, the striking similarity between the murine and human disorders provokes speculations on a common defect downstream of the bcr–abl signaling pathway.

Approximately 75% of patients in chronic stage of CML achieve hematologic remission after IFNα therapy. It has been previously discussed that IFN might counteract the enhanced proliferation of leukemic cells by blocking the signaling pathways of growth factors, thus allowing normal maturation to continue (Gutterman, 1994). The notion that IFN regulates proliferation of hematopoietic cells has been substantiated by Hwang et al. (1995), who found elevated levels of myeloid lineage cells in peripheral blood and bone marrow of IFNα-receptor deficient mice. Thus, it is not entirely surprising that the disruption of ICSBP gene connected with an alteration of IFN signaling is manifested by an enhanced cell proliferation. It is conceivable that the absence of ICSBP (and IRF-2) leads to a disequilibrium of IRF and IRF–interacting proteins (STATs, Pu.1) with a consequent formation of different protein complexes that in turn activate other target genes. Taken together, the data suggest that the balance between proliferative (growth factors) and antiproliferative (IFN) signals is maintained by interactions of STAT and IRF factors.

Similar to human CML, ICSBP$^{-/-}$ and, with a lower frequency, ICSBP$^{+/-}$ mice transit from a chronic stage to acute blast crisis characterized by clonal expansion of leukemic cells. Prolonged cell survival allowing time for additional mutations in other oncogenes is the most likely mechanism to explain transition of chronic to acute blastic leukemia (Rabbitts, 1991, 1994). It would be interesting to study whether the same gene alterations as those described in humans are involved also in the ICSBP leukemia.

The results shown argue for an essential role of ICSBP in the differentiation of hematolymphoid cells. However, the mechanisms leading to leukemic transformation, the signaling intermediates and target genes that are deregulated in ICSBP–deficient mice, remain to be determined. The ICSBP–deficient mice should be a valuable tool to study the signaling pathways that control normal and malignant proliferation of hematolymphoid cells.

Experimental Procedures

Targeting Vector

To generate the targeting vector, phage clones containing ICSBP genomic sequences were isolated from a mouse BALB/c DNA library (Driggers et al., 1992). The clone used encompasses the second exon and first and second intron of ICSBP gene. The PGK-neo cassette (Rudnicki et al., 1992) was introduced in the sense orientation into the unique SmaI site of the second exon. The PGK-tk cassette was introduced into ScaI site 3′ of the homologous ICSBP sequence. The final targeting vector pPNS-icsbp contains 4.0 of ICSBP homology and can be linearized by PvuI.

Transfection of Embryonic Stem Cells and Blastocyst Injection

Linearized pPNAS-icsbp DNA (1.5 μg) was electroporated into E14.1 embryonic stem cells (Schorle et al., 1991), and embryonic stem–cell clones were grown under double selection as described (Rudnicki et al., 1992). DNA of individual double-resistant clones was cut with BamHI and probed with A and B probes. The screening strategy and probes are shown in Figure 1. Homologous recombinant clones demonstrated a 3.5 kb recombinant band, in addition to a 5.0 kb wild-type band in Southern blots. Alternatively, PCR analysis was employed to distinquish the mutated and wild-type allele. The sequences of the three primers are: first, 5′-CATGGCACTGGTCC AGATGTCTTCC-3′; second, 5′-CTTCCAGGGGATACGGAACATG GTC-3′; and third, 5′-CGAAGGAGCAAAGCTGCTATTGGCC-3′. Positive clones were expanded and injected into C57BL/6 blastocysts. Resulting chimeric animals were crossed to both C57BL/6 and 129/Ola mice. Germline transmission was identified by Southern blotting, and brother–sister mating was carried out to generate ICSBP$^{-/-}$ mice. Mice were kept in barrier facilities.

Electrophoretic Mobility Shift Assay and Immunoblot Analysis

Nuclear extracts were prepared according to Antalis and Godbolt (1991), with a modified lysis buffer that contained 10 mM Tris (pH 7.5), 10 mM NaCl, 15 mM $MgCl_2$, 0.05% NP40, and protease inhibitors (Boehringer Manheim). Reactions for electrophoretic mobility shift assay were performed as described (Kanno et al., 1993), using 10 μg of nuclear extract. The ISRE probe was from the ISG15 gene (Bovolenta et al., 1994), and the NFκB probe was from the Igk gene.

Immunologic Procedures

Samples from tissues were frozen at -70°C in RNAzol for later processing in RT–PCR analyses, and single cell suspensions were prepared from lymphoid organs for tissue culture and FACS analyses. Cells were stained with monoclonal antibodies (MAbs) prepared in our laboratory or purchased from Pharmingen, labeled with FITC, phycoerythrin, or biotin. The biotin-labeled antibodies were detected using avidin coupled to FITC, phycoerythrin, or allophycocyanin. The MAbs included those to CD4, CD5, CD8, CD11b (Mac-1), CD32, CD45R(B220), CD54(ICAM-1), MHC class I H-$2K^b$, MHC class II I-Ab, TCRα/β, and GR-1. Viable cells gated by narrow forward-angle light scatter and exclusion of propidium iodide were analyzed on a FACScan or a FACS Vantage (Becton Dickinson) using Cellquest software.

In studies of IFNγ induction, cells were cultured in 1 ml volumes in 24 well plates at 5×10^6 cells/ml. Supernatants were harvested at 24–72 hr after stimulation with ConA (5 μg/ml), LPS (50 μg/ml), and plate-bound anti–TCRα/β monoclonal antibody (300 ng/well), and assayed for IFNγ levels using an enzyme-linked immunosorbent assay as previously described (Gazzinelli et al., 1993).

The primers, probes, and methods for preparation of RNA, cDNA, and amplification of cytokine transcripts were as previously described (Giese et al., 1996).

Antiviral Immune Responses

Viruses: VSV (serotype Indiana, Mudd-Summers isolate) was originally obtained from D. Kolakowsky (University of Geneva); VV (WR isolate) was obtained from B. Moss (National Institutes of Health, Bethesda, Maryland). LCMV isolate WE was from F. Lehmann-Grube (Hamburg) and isolate Armstrong from M. B. A. Oldstone (Scripps Clinic, La Jolla, California).

Primary CTL activity ex vivo: $ICSBP^{-/-}$ mice and their normal littermates were infected with 2×10^6 pfu of VV or with 2×10^2 pfu of LCMV. On day 6 (VV) or 8 (LCMV), effector spleen cell suspensions were prepared and diluted to 9×10^6 cells/ml in MEM supplemented with 2% FCS. Serial 3-fold dilutions of effector cells were assayed in 96 well plates. In vitro VV–infected MC57 or LCMV gp33 peptide-labeled EL4 target cells were incubated for 120 min in 0.2 ml of ^{51}Cr-containing medium and assayed as described previously (Huang et al., 1993).

Secondary CTL activity in vitro: $ICSBP^{-/-}$ mice and their normal littermates were infected with 2×10^6 pfu of VSV or 2×10^2 pfu of LCMV. On day 30 (VSV) or day 40 (LCMV), effector spleen cell suspensions ($3–4 \times 10^6$) were cocultured with stimulator cells (1×10^6), pulsed with the appropriate peptide, and irradiated with 2000 rad. On day 5, ^{51}Cr-release assay on peptide-labeled target cells was performed as described.

Histologic and Immunohistologic Methods

Tissue specimens were fixed in either 4% formaldehyde/1% acetic acid or Bouin's fixative or were snap-frozen for cryostat sectioning. Sections were stained with hematoxylin-eosin, periodic acid-Schiff reaction, or Giemsa and Van-Gieson stain. Blood films and bone marrow smears were fixed with methanol and stained with May-Grünwald and Giemsa solution. To demonstrate immunoglobulins, myeloperoxidase, and lysozyme in paraffin sections by the avidin-biotin-peroxidase or alkaline-phosphatase method (Hsu et al., 1981), we used polyclonal rabbit anti-mouse κ and λ light chain, α, γ, and ϵ heavy chain (Nordic), goat anti-mouse μ heavy chain, rabbit anti-human myeloperoxidase (DAKO), and anti-human lysozyme (Biogenex) antibodies. The immunostaining was performed with a panel of rat monoclonal antibodies directed against lineage-specific differentiation antigens: Thy-1.2, I-A, Mac-1 (ATCC), CD3, B220, MOMA-2 (Serotec), Gr-1, and ER-MP (Pharmingen). As secondary overlays, biotin-conjugated F(ab')2 fragments of immunoaffinity-purified sheep anti-rabbit IgG (Sigma), rabbit anti-goat IgG, or goat anti-rat IgG (Dianova) were employed and subsequently detected with streptavidin-biotinylated peroxidase complexes (DAKO) or "supersensitive" streptavidin-alkaline phosphatase conjugate (Biogenex). Peroxidase activity was revealed with H_2O_2 and 3,3-diaminobenzidine-tetrahydrochloride (Fluka).

Cell Transfers

Cells from organs of donor mice were suspended, washed, and injected intravenously into tails of 2–6-month-old recipient mice (C57BL/6 $\times$ 129/Ola) F_1 mice. Mice were monitored twice a week and were killed for histopathologic studies and collection of tissues for mRNA and DNA analyses when moribund.

Acknowledgments

We thank S. Chattopadhyay for help with clonality assay and H. Haber, K. Heigl, Y. Kim, N. Nelson, and A. Peters for technical assistance. These studies were supported by grants from the Deutsche Forschungsgemeinschaft (SFB 465) and the Sander-Stiftung to I. H. and by Human Science Frontier Program Strassburg and the Swiss National Science Foundation to R. M. Z. The Heinrich-Pette-Institute is supported by Freie und Hansestadt Hamburg and Bundesministerium für Gesundheit, Bonn. J. W. was supported by A. von Humboldt Foundation and L. G. in part by the AIDS Italian National Project. Correspondence should be sent to I. H. (fax: ++49-30-8445-3803).

Received April 22, 1996; revised August 9, 1996.

References

Antalis, T.M., and Godbolt, D. (1991). Isolation of intact nuclei from hematopoietic cell types. Nucl. Acids Res. *19*, 4301.

Au, W.-C., Moore, P.A.. Lowther, W., Juang, Y.-T., and Pitha, P.M. (1995). Identification of a member of the interferon regulatory factor family that binds to the interferon-stimulated response element and activates expression of interferon-induced genes. Proc. Natl. Acad. Sci. USA *92*, 11657–11661.

Bovolenta, C., Driggers, P.H., Marks, M.S., Medin, J.A., Poltis, A.D., Vogel, S.N., Levy, D.E., Sakaguchi, K., Appella, E., Coligan, J.E., and Ozato, K. (1994). Molecular interactions between interferon consensus sequence binding protein and members of the interferon regulatory factor family. Proc. Natl. Acad. Sci. USA *91*, 5046–5050.

Carlesso, N., Frank, D., and Griffin, J.D. (1996). Tyrosyl phosphorylation and DNA binding activity of signal transducers and activators of transcription (STAT) proteins in hematopoietic cell lines transformed by bcr/abl. J. Exp. Med. *183*, 811–820.

Danial, N.N., Pernis, A., and Rothman, P.B. (1995). Jak–STAT signaling induced by the v-abl oncogene. Science, *269*, 1875–1877.

Darnell, J.D., Jr., Kerr, I.M., and Stark, G.R. (1994). Jak–STAT pathways and transcriptional activation in response to IFN and other extracellular signaling proteins. Science *264*, 1415–1421.

Driggers, P.H., Elenbaas, B.A., An, J.-B., Lee, I.J., and Ozato, K. (1992). Two upstream elements activate transcription of major histocompatibility complex class I gene in vitro. Nucl. Acids Res. *20*, 2533–2540.

Eisenbeis, C.F., Singh, H., and Storb, U. (1995). Pip, a novel IRF family member, is a lymphoid-specific, PU.1-dependent transcriptional activator. Genes Dev. *9*, 1377–1387.

Gazzinelli, R.T., Hieny, S., Wynn, T.A., Wolf, S., and Sher, A. (1993). Interleukin 12 is required for the T-lymphocyte–independent induction of interferon γ by an intracellular parasite and induces resistance in T-cell–deficient mice. Proc. Natl. Acad. Sci. USA *90*, 6115–6119.

Giese, N.A., Gazzinelli, R.T., Actor, J.K., Morawetz, R.A., and Morse, H.C., III. (1996). Retrovirus-elicited interleukin-12 and tumour necrosis factor-α as inducers of interferon-γ–mediated pathology in mouse AIDS. Immunology *87*, 467–474.

Gutterman, J.U. (1994). Cytokine therapeutics: lessons from interferon α. Proc. Natl. Acad. Sci. USA *91*, 1198–1205.

Harada, H., Fujita, T., Miyamoto, M., Kimura, Y., Marayama, M., Furia, A., Miyata, T., and Taniguchi, T. (1989). Structurally similar but functionally distinct factors, IRF-1 and IRF-2, bind to the same regulatory elements of IFN and IFN-inducible genes. Cell *58*, 729–739.

Harada, H., Kitagawa, M., Tanaka, N., Yamamoto, H., Harada, K., Ishihara, M., and Taniguchi, T. (1993). Anti-oncogenic and oncogenic potentials of interferon regulatory factors-1 and -2. Science *259*, 971–974.

Hawley, R.G., Fong, A.Z.C., Burns, B.F., and Hawley, T.S. (1992). Transplantable myeloproliferative disease induced in mice by an interleukin 6 retrovirus. J. Exp. Med. *176*, 1149–1163.

Hsu, S.M., Raine, L., and Fanger, H. (1981). Use of avidin–biotin–peroxidase complex (ABC) in immunoperoxidase techniques: a comparison between ABC and unlabeled antibody (PAP) procedure. Hisochem. Cytochem. *29*, 577–580.

Huang, S., Hendriks, W., Althage, A., Hemmi, S., Bluethmann, H., Kamijo, R., Vilcek, J., Zinkernagel, R.M., and Aguet, M. (1993). Immune response in mice that lack the interferon-gamma receptor. Science *259*, 1742–1745.

Hwang, S.Y., Hertzog, P.J., Holland, K.A., Sumarsono, S.H., Tymms, M. J., Hamilton, J.A., Whitty, G., Bertoncello, I., and Kola, I. (1995). A null mutation in the gene encoding a type I interferon receptor component eliminates antiproliferative and antiviral responses to interferons α and β and alters macrophage responses. Proc. Natl. Acad. Sci. USA *92*, 11284–11288.

Johnson, G.R., Gonda, T.J., Metcalf, D., Hariharan, I.K., and Cory, S. (1989). A lethal myeloproliferative syndrome in mice transplanted with bone marrow cells infected with a retrovirus expressing granulocyte-macrophage colony stimulating factor. EMBO J. *8*, 441–448.

Kanno, Y., Kozak, C.A., Schindler, C., Driggers, P.H., Ennist, D.L., Gleason, S.L., Darnell, J.E., Jr., and Ozato, K. (1993). The genomic structure of the murine ICSBP gene reveals the presence of the gamma interferon-responsive element, to which an ISGF3α subunit (or similar) molecule binds. Mol. Cell. Biol. *13*, 3951–3963.

Maniatis, T., Whittemore, L., Du, W., Fan, C., Keller, A.D., Palombella, V.J., and Thanos, D.N. (1992). Positive and negative control of interferon-β gene expression. In Transcription Regulation, S.L. McKnight and K.R. Yamamoto, eds. (Cold Spring Harbor, New York: Cold Spring Harbor Laboratory Press), pp. 1193–1220.

Matsuyama, T., Kimura, T., Kitagawa, M., Pfeffer, K., Kawakami, T., Watanabe, N., Kündig, T.M., Amakawa, R., Kishihara, K., Wakeham, A., Potter, J., Furlonger, C.L., Naredran, A., Suzuki, H., Ohashi, P.S., Paige, C.J., Taniguchi, T., and Mak, T.W. (1993). Targeted disruption of IRF-1 or IRF-2 results in abnormal type I IFN gene induction and aberrant lymphocyte development. Cell *75*, 83–97.

Metcalf, D. (1989). The molecular control of cell division, differentiation commitment and maturation in hemopoietic cells. Nature *339*, 27–30.

Miyamoto, M., Fujita, T., Kimura, Y., Maruyama, M., Harada, H., Sudo, Y., Miyata, T., and Taniguchi, T. (1988). Regulated expression of a gene encoding a nuclear factor, IRF-1, that specifically binds to IFN-β gene regulatory elements. Cell *54*, 903–913.

Moskophidis, D., Lechner, F., Pircher, H.P., and Zinkernagel, R.M. (1993). Virus persistence in acutely infected immunocompetent mice by exhaustion of antiviral cytotoxic effector T cells. Nature *362*, 758–761.

Müller, U., Steinhoff, U., Reis, L.F.M., Hemmi, S., Pavlovic, J., Zinkernagel, R.M., and Aguet, M. (1994). Functional role of type I and type II interferons in antiviral defense. Science *264*, 1918–1921.

Nelson, N., Marks, M.S., Driggers, P.H., and Ozato, K. (1993). Interferon consensus sequence-binding protein, a member of the interferon regulatory factor family, suppresses interferon-induced gene transcription. Mol. Cell. Biol. *13*, 588–599.

Nelson, N., Kanno, Y., Hong, C., Contursi, C., Fujita, T., Fowlkes, B.J., O'Connell, E., Hu-Li, J., Paul, W.E., Jankovic, D., Sher, A.F., Coligan, J.E., Thornton, A., Appella, E., Yang, Y., and Ozato, K. (1996). Expression of interferon regulatory factor family proteins in lymphocytes: induction of Stat 1 and ICSBP expression by T cell activation. J. Immunol. *156*, 3711–3720.

Palombella, V.J., and Maniatis, T. (1992). Inducible processing of interferon regulatory factor-2. Mol. Cell. Biol. *12*, 3325–3336.

Pine, R., Canova, A., and Schindler, C. (1994). Tyrosine phosphorylated p91 binds to single element in the ISGF.IRF-1 promoter to mediate induction by IFNα and IFNγ, and is likely to autoregulate the p91 gene. EMBO J. *13*, 158–167.

Rabbitts, T.H. (1991). Translocations, master genes and differences between the origins of acute and chronic leukemias. Cell *67*, 641–644.

Rabbitts, T.H. (1994). Chromosomal translocations in human cancer. Nature *372*, 143–149.

Rudnicki, M.A., Braun, T., Hinuma, S., and Jaenisch, R. (1992). Inactivation of MyoD in mice leads to up-regulation of the myogenic HLH gene Myf-5 and results in apparently normal muscle development. Cell *71*, 383–390.

Sawyers, C.L., Denny, C.T., and Witte O.N. (1991). Leukemia and the disruption of normal hematopoiesis. Cell *64*, 337–350.

Schorle, H., Holtschke, T., Hünig, T., Schimpl, A., and Horak, I. (1991). Development and function of T cells in mice rendered interleukin-2 deficient by gene targeting. Nature *352*, 621–624.

Shivdasani, R.A., and Orkin, S.H. (1996). The transcriptional control of hematopoiesis. Blood *87*, 4025–4039.

Thornton, A.M., Buller, R.M., DeVico, A.L., Wang, I.-M., and Ozato, K. (1996). Inhibition of HIV and vaccinia virus infection by a dominant negative factor of the IRF family expressed in monocytic cells. Proc. Natl. Acad. Sci. USA *93*, 383–387.

Trinchieri, G. (1995). Interleukin-12: a proinflammatory cytokine with immunoregulatory functions that bridge innate resistance and antigen-specific adaptive immunity. Annu. Rev. Immunol. *13*, 251–276.

Veals, S.A., Schindler, C., Leonard, D., Fu, X.-Y., Aebersold, R., Darnell, J.E., Jr., and Levy, D.E. (1992). Subunit of an alpha-interferon–responsive transcription factor is related to interferon regulatory factor and Myb families of DNA-binding proteins. Mol. Cell. Biol. *12*, 3315–3324.

Weissman, I.L. (1994). Stem cells, clonal progenitors, and commitment to the three lymphocyte lineages: T, B, and NK cells. Immunity *1*, 529–531.

Wong, P.M.C., Chung, S.-W., Dunbar, C.E., Bodine, D.M., Ruscetti, S., and Nienhuis, A.W. (1989). Retrovirus-mediated transfer and expression of the interleukin-3 gene in mouse hematopoietic cells results in a myeloproliferative disorder. Mol. Cell. Biol. *9*, 798–808.

Zinkernagel, R.M., Haenseler, E., Leist, T.P., Cerny, A., Hengartner, H., and Althage, A. (1986). T cell mediated hepatitis in mice infected with lymphocytic choriomeningitis virus. J. Exp. Med. *164*, 1057–1092.